1 **Identifying transcriptomic downstream targets of genes commonly mutated in**

2 **Hereditary Hemorrhagic Telangiectasia**

3

4 Md Khadem Ali[1,2], Yu Liu[3,4], Katharina Schimmel[l,2,3], Nicholas H. Juul[5], Courtney A.

5 Stockman[5], Joseph C. Wu[3,4,6], Edda F. Spiekerkoetter[1,2, *]

6

7 [1]Department of Medicine, Division of Pulmonary, Allergy and Critical Care Medicine,

8 Stanford University, Stanford, CA, USA

9 [2]Vera Moulton Wall Center for Pulmonary Vascular Disease, Stanford University, Stanford,

10 CA, USA

11 [3]Stanford Cardiovascular Institute, Stanford University School of Medicine, Stanford, CA,

12 USA

13 [4]Division of Cardiovascular Medicine, Department of Medicine, Stanford University School

14 of Medicine, Stanford, CA, USA

15 [5]Institute for Stem Cell Biology and Regenerative Medicine, Division of Pulmonary Allergy

16 and Critical Care Medicine

17 [6]Molecular Imaging Program at Stanford, Department of Radiology, Stanford University

18 School of Medicine, Stanford, CA, USA

19

20 *Corresponding author:

21 Edda Spiekerkoetter, MD

22 Associate Professor of Medicine

23 Division of Pulmonary, Allergy and Critical Care Medicine

24 Vera Moulton Wall Center for Pulmonary Vascular Disease

25 Stanford University

26 300 Pasteur Drive

27 Stanford, CA 94305, USA

28 Phone: +1 (650) 739-5031

29 Email: eddas@stanford.edu

30

31

32

33

34

35 **Abstract**

36 Hereditary Hemorrhagic Telangiectasia (HHT) is an autosomal dominant disease that causes

37 arteriovenous vascular malformations (AVMs) in different organs, including the lung. Three

38 genes, ENG (endoglin), ACVRL1 (ALK1) and SMAD4, all members of the TGF-β/BMPR2

39 signaling pathway, are responsible for over 85% of all HHT cases. However, how these loss-

40 of-function gene mutations lead to AVMs formation and what common downstream

41 signaling they target is unknown. Here, using a combination of siRNA-mediated gene

42 silencing, whole transcriptomic RNA sequencing, bioinformatic analysis, transcriptomic-

43 based drug discovery, endothelial cells functional assays and VEGF signaling analysis, and

44 *ex vivo* precision cut lung slice (PCLS) cultures approach, we uncovered common

45 downstream transcriptomic gene signatures of HHT-casing genes and identified promising

46 drug for HHT. We found the commonly used BMPR2-signaling downstream target ID1 is not

47 a common downstream target of all the three HHT genes knockdown in human pulmonary

48 microvascular endothelial cells (PMVECs). We identified novel common downstream targets

49 of all the three HHT-causing genes that were enriched for HHT-related biological process

50 and signaling pathways. Among those downstream genes, LYVE1, GPNMB, and MC5R

51 were strong downstream targets that could serve as a better common downstream target than

52 ID1. Furthermore, using the common downstream upregulated genes (HHT disease signature)

53 following HHT gene knockdown, we identified a small molecule drug, Brivanib, that

54 reversed the HHT disease signature, and inhibited VEGF-induced ERK1/2 phosphorylation,

55 proliferation, and angiogenesis in PMVECs and inhibited some of the upregulated HHT

56 disease genes in PCLS. Our findings suggest that Brivanib could be an emerging new drug

57 for HHT.

58

59 **Keywords:** Pulmonary arteriovenous malformation, hereditary hemorrhagic telangiectasia,

60 pulmonary microvascular endothelial cells, angiogenesis, drug repurposing

61

62

63 **Introduction**

64 Hereditary hemorrhagic telangiectasia (HHT), also known as Rendu-Osler-Weber syndrome,

65 is a complex genetic disease that causes abnormalities of blood vessel formation in the liver,

66 lung, brain, skin, nasal mucosa, and gastrointestinal tract [1]. HHT is a rare disease, affecting

67 approximately 1 in 5000-10000 people worldwide [2]. The key cardinal clinical

68 manifestations of the disease include epistaxis (nose bleeding, present in 90% of cases),

69   gastrointestinal hemorrhage, mucocutaneous telangiectasias (blood vessel dilations), and

70   visceral arteriovenous malformations (AVMs). Clinically, HHT is generally diagnosed based

71   on the four established Curacao Criteria; recurrent epistaxis, telangiectasia, family history,

72   and visceral AVMs [3]. The diagnosis of HHT is confirmed when three or more criteria are

73   met, while it is suspected if just two criteria are fulfilled. AVMs are large abnormal

74   connections between arteries and veins bypassing the capillaries and result in severe bleeding

75   when present in the nose, GI tract, and brain or cause paradoxical emboli and stroke when

76   present in the lungs. AVMs in the lung (15-45%) and liver (>70%) are most common, while

77   brain AVMs develop in 10-23% of HHT patients [4]. Currently, HHT therapies aim to lessen

78   the disease's symptoms. However, there is currently no mechanism-based targeted therapy

79   available.

80

81   The majority (about >85%) of the HHT patients have loss of function mutations in either

82   ENG (HHT type 1) or ACVRL1 (ALK1) (HHT type 2), but a small percentage of them

83   (approximately <1%) have mutations in SMAD4 causing the combined juvenile

84   polyposis/HHT syndrome. Interestingly, all three HHT-causing genes encode proteins

85   belonging to the same TGFß superfamily of proteins. All three HHT gene products function

86   in SMAD-dependent signaling pathways in which the activated Smad complex enters the cell

87   nucleus and regulates transcriptional programs. Previous *in vivo* studies showed that any of

88   the three HHT gene mutations could cause vascular malformations since knockout alleles for

89   ENG, ACVRL1, and SMAD4 all result in HHT-like phenotypes in mice [1]. Mechanistically,

90   in addition to the TGFß/BMP pathway, several other pathways, such as VEGF, mTOR, and

91   PI3K/AKT signaling pathways, are associated with AVM formation and HHT pathogenesis

92   [1]. Recently, pharmacologically combined treatment with Sirolimus and Nintedanib has

93   been shown to correct Smad1/5/8 reduction and mTOR and VEGFR2 activation. This

94   combination drug treatment reversed and prevented vascular abnormalities, bleeding and

95   associated anemia in two experimental HHT mouse models (BMP9/10i antibody-, and the

96   inducible ALK1 knock out mouse model of HHT) [5].

97

98   One of the known downstream targets of BMPR2/ALK1 signaling are the inhibitors of DNA-

99   binding/differentiation proteins (IDs). ID proteins are thought to inhibit differentiation and

100   promote cell cycle progression, to be involved in venous, arterial, and lymphatic endothelial

101   cell identify and, therefore, when dysregulated, could possibly explain the aberrant

102   proliferation observed during AVM pathogenesis in HHT[6]. In support of this, mice with a

103   combined loss of both *Id1* and *Id3* display cranial hemorrhage secondary to the formation of

104   an anastomosing network of dilated capillaries in the brain[7], suggesting that ID1/3 may

105   play a role in AVM formation. Our group has previously identified the repurposed drugs

106   Tacrolimus (FK506) and Enzastaurin as "ID1-increasing" drugs, which improved endothelial

107   function *in vitro* [8, 9] as well as prevented and reversed the occlusive vasculopathy in

108   pulmonary hypertension, a second rare disease characterized by haploinsufficiency in the

109   BMPR2/ALK1 signaling pathway. FK506 was identified in a High Throughput Screen (HTS)

110   of FDA-approved drugs using Id1 expression as a readout, whereas Enzastaurin was

111   identified in a combined approach, using an siRNA screen (HTS) as well as *in silico* drug

112   prediction of candidates that reverse the "transcriptomic disease signature" derived from

113   blood cells from patients with pulmonary arterial hypertension (PAH). FK506 was used in an

114   early proof of concept trial initiated at Stanford University [10] in stable PAH patients and

115   improved outcomes when used as compassionate therapy in end-stage PAH patients [11].

116

117   Furthermore, low-dose FK506 attenuated nose bleeding in patients with HHT and PAH [12].

118   It was able to block the retinal pathology characterized by robust hypervascularization and

119   AVM development in animal models of HHT[13]. While FK506 (and potentially

120   Enzastaurin) might be beneficial in reducing AVM complications in HHT, we are proposing,

121   that ID1 might not be the most specific readout for the dysfunctional ALK1/ENG/SMAD

122   signaling in HHT, and therefore not the best target for drug repurposing efforts in HHT. The

123   phenotypes of HHT (enlarged vascular malformations) and PAH (occlusive vasculopathy) are

124   quite different, suggesting a different "gene expression signature" in HHT and PAH.

125   Furthermore, given the complexity of the BMPR2/ALK1 pathway, including receptor

126   heterodimerization, finely orchestrated ligand binding as well as interactions with other

127   signaling pathways, mutations in BMPR2, as observed in PAH, likely do not result in the

128   exact same signaling disturbances as mutations in ENG, ALK1 or SMAD4.

129

130   Since the three HHT-causing genes (ENG, ALK1, SMAD4) are responsible for the same

131   phenotype, AVM formations, albeit with a different frequency and location in visceral organs

132   depending on the specific mutation, it would be very important to identify downstream

133   signaling abnormalities that are common to all three loss-of function mutations. The ultimate

134   goal would be to identify ways to restore normal signaling and improve AVMs. Current

135   therapies for large visceral AVMs in HHT are limited and consist of catheter-directed

136   embolization or surgery, but no treatment exists that restores normal signaling. Drugs applied

137 systemically that could restore normal signaling might prevent the development and growth

138 of existing AVMs, an approach particularly important for children with HHT whose small

139 AVMs grow with age. Furthermore, this approach might benefit patients with multiple

140 smaller AVMs (in the lungs, nose, GI tract) and severe hypoxia, bleeding, and subsequent

141 anemia, whose AVMs are not amenable to embolization because of their size and number but

142 might respond to medical therapy, as has been shown with anti-angiogenic therapies

143 including the use of VEGF inhibitors such as Bevacizumab for severe anemia[14]. Our study

144 has two aims: *First*, to identify common downstream genes and signaling pathways of the

145 three known HHT-causing gene mutations (ALK1, ENG, SMAD4) using siRNA mediated

146 gene downregulation, thereby mimicking complete local loss of function as seen in AVMs in

147 HHT patients [15]. *Second,* to identify repurposed/novel drugs that reverse the dysfunctional

148 transcriptomic gene expression signature and normalize downstream signaling. We found that

149 ID1 is not a common downstream target of all the three HHT gene mutations in PMVECs,

150 and identified LYVE1, GPNMB, MC5R, and PLXDC2 as downstream targets of all three

151 HHT genes. Importantly, we discovered a small molecule drug, Brivanib, that can activate

152 downstream targets of ALK1/ENG/SMAD4 signaling, inhibit VEGF signaling pathways, and

153 improve PMVECs functions.

154

155

156 **Methods:**

157 **Cell culture:** Human healthy control pulmonary microvascular endothelial cells (PMVECs)

158 (Cat # C12281, PromoCell GmbH, Heidelberg, Germany) were cultured in microvascular

159 endothelial cell basal media (Cat # C-22120; PromoCell GmbH) supplemented with growth

160 factors (Growth Medium MV SupplementPack, Cat # C-39220, PromoCell GmbH) and 100

161 U/mL Penicillin-Streptomycin Solution (Gibco) and used between passages 4 to 8. PMVECs

162 were cultured under standard conditions (37°C, 5% CO_2, 21% O_2, 90% humidity).

163

164 **RNAi.** Human pulmonary microvascular endothelial cells of passages 4-6 were seeded at

165 150K cells/well onto 6-well plates and incubated at 37ºC in a humidified 5% CO2

166 atmosphere. The next day, cells were washed with PBS and transfected with 50nM siRNAs

167 against non-target controls, ACVRL1 (ALK1), ENG, SMAD4, LYVE1, GPNMB or MC5R

168 (Thermo Fisher Scientific, Waltham, MA), and 2ul of Lipofectamine RNAiMAX in a total

169 1ml of OPTIMEM media. After 5 hrs of transfection, the medium was replaced with regular

170 complete growth media. The following day, a starvation medium (0.2% FCS media) was

171   added and incubated for 16 hrs. Cells were then stimulated with 20ng/ml of BMP9 for 2 or 24

172   hrs, harvested for RNA isolation, and performed RNAseq analysis.

173

174   **RNA sequencing (RNAseq)**. RNA was isolated using RNeasy Plus Kits (Qiagen,

175   Gaithersburg, MD) as per the manufacturer's instructions. RNA samples were sent to the

176   Novogene Corporation (Sacramento, CA), where the following steps were carried out:

177   **Quality control:** Quality and integrity of total RNA were controlled on Agilent Technologies

178   2100 Bioanalyzer (Agilent Technologies; Waldbronn, Germany). The RIN values of all

179   samples were in the ranges between 9.9-10. **Library construction:** The RNA sequencing

180   library was constructed using NEBNext® Ultra II RNA Library Prep Kit (New England

181   Biolabs) according to the manufacturer's protocols. **Library quality control:** Library

182   concentration was quantified using a Qubit 2.0 fluorometer (Life Technologies) and then

183   diluted to 1ng/ul before checking insert size on an Agilent Technologies 2100 Bioanalyzer

184   (Agilent Technologies; Waldbronn, Germany). The library was then quantified to greater

185   accuracy by quantitative PCR (qPCR). **Sequencing:** 30 million paired reads for each sample

186   were acquired with the Illumina NovaSeq 6000 system (Q20% (97-98%), Q30% (94-96%),

187   GC content % (50-52%). **Data analysis**. The quality of the RNA-seq data was examined by

188   base sequence quality plots using FastQC. TrimGalore was used to trim the sequence reads.

189   Then, the RNA-seq reads were aligned to the human genome (hg19) using the STAR

190   software, and a gene database was constructed from Genecode v19. Differentially expressed

191   genes (DEG) between groups were quantified using the DESeq2 R package.

192

193   **Biological process, pathway enrichment, and protein-protein network analysis:**

194   Differentially expressed downstream genes of HHT knock-down (KD) conditions at 2 and

195   24h of BMP9 stimulations were uploaded on the ShinyGO 0.76

196   (http://bioinformatics.sdstate.edu/go/) platform to analyze GO biological process enrichment.

197   The same data gene signatures were uploaded separately onto the DAVID Bioinformatics

198   Resources 6.8 server (https://david.ncifcrf.gov/summary.jsp) for GO pathway enrichment

199   analysis. The identifier was set to gene symbol, and *Homo sapiens* was selected to limit

200   annotations in the gene list and background list. A significant value of $p < 0.05$ was set as the

201   cutoff criterion. STRING Network analysis was performed using the SinyGO 0.76 platform.

202

203   *In silico* **Drug prediction:** Following knockdown of the HHT-causing genes (ALK1, ENG,

204   SMAD4) in PMVECs, we performed RNAseq and defined gene expression changes common

205   to silencing of the three HHT-causing genes as "disease signature". We then used the

206   common downstream gene signature of all **up-**regulated genes 117 and 112 following HHT

207   gene knockdown and at 2 and 24 h of BMP9 stimulation for drug prediction. Using the Broad

208   Institute's Clue.io query app https://clue.io/query, we identified compounds that reverse the

209   common HHT disease signature of up-regulated genes. The list of up-regulated genes 117

210   (2h) and 112 (24h) genes following RNAseq was uploaded separately on the app

211   https://clue.io/query, selecting with the gene expression L1000 query parameter. This web-

212   based clue.io query app finds perturbagens that give rise to similar (or opposing) expression

213   signatures. After running this query, we identified compounds that either mimic the

214   transcriptional disease signature (compounds that could potentially worsen disease) or mimic

215   the anti-signature (compounds that could potentially improve disease) in different cell lines.

216   We only focused on findings from the human umbilical vein endothelial cells (HUVECs)

217   data sets as this was the only dataset performed in endothelial cells, which are the critical cell

218   type for AVM formation[16]. Top-ranked 5 CMAP compounds/drugs induced transcriptome

219   alterations oppositional to (indicated by negative similarity mean) or overlapping with

220   (indicated by positive similarity mean) caused by HHT causing gene knockdowns. Rank was

221   determined by samples n>=3, tas value >=0.20, normalized connectivity score, and FDR

222   value. Next, we narrowed down the top scoring drug list based on their relevance to VEGF

223   inhibition as VEGF signaling is overactivated in HHT.

224

225   **Cell proliferation, apoptosis, and tube formation assay.** MTT assay (Cat # V13154,

226   Invitrogen, Waltham, MA), and caspase-3/7 assay (Cat # G8090, Promega, Madison, WI)

227   were performed using commercially available kits as per the instructions to assess

228   proliferation and apoptosis, respectively.

229

230   **Matrigel tube formation assay.** The bottom of a 96-well plate was coated with 50ul per well

231   of Matrigel and incubated at 37 °C for 1 h. PMVECs (1×10^4 cells/100 µl per well)

232   suspended in a starvation medium were added to the Matrigel and cultured at 37 °C and 5%

233   CO_2 for 5 h. Vessel tube-like structures were observed and photographed under a

234   microscope with a digital imaging system. The data were analyzed using ImageJ with an

235   angiogenesis analyzer tool.

236

237   **RNA isolation, RT-PCR, and qRT-PCR:** Total RNA was isolated from cells using a

238   commercially available RNeasy® Plus Mini Kit (Cat # 74134, Qiagen, Hilden, Germany).

239 For precision cut lung slices (PCLS), total RNA was extracted and purified using the TRizol

240 RNA extraction protocol, as described previously [17]. The total RNAs were then converted

241 to cDNA using a commercially available high-capacity cDNA Reverse Transcription Kit (Cat

242 # 4368813, Applied Biosystems^{TM}, Foster City, CA) according to the manufacturer's

243 instructions. The expression levels of mRNAs were quantified using TaqMan™ 2x Universal

244 PCR Master Mix (Cat # 4304437) and targeted Taqman probes (ALK1, ENG, SMAD4,

245 GAPDH, Hs02786624_g1; ID1, Hs03676575_s1; HS3ST2, Hs00428644_m1; GPNMB,

246 Hs01095679_m1; ANKRD33, Hs05002807_s1; RRAGD, Hs00222001_m1; LYVE1,

247 Hs00272659_m1; CPA4, Hs01040939_g1; SLC25A47, Hs01584239_m1; SHISA9,

248 Hs04188640_m1; HIST1H2BE, Hs00543841_s1; MC5R, Hs00271882_s1; FGF19,

249 Hs00192780_m1; FRG2C, Hs01695863_sH; PLXDC2, Hs00262350_m1; KCNK5,

250 Hs01123564_m1; and CACNA1G, Hs00367969_m1, Thermo Fisher Scientific, Waltham,

251 MA) and normalized to a housekeeping control GAPDH.

252

253 **Western blot.** Western blotting was carried out as described previously[8, 18]. The following

254 antibodies were used: P-Smad1/5/9 (Cat # CST13820S, 1:1000), p44/42 MAPK (Erk1/2)

255 (137F5) (ERK1/2 MAPK) (Cat # CST4695S, 1:1000), phosphorylated ERK1/2 (Phospho-

256 p44/42 MAPK (Erk1/2) (Thr202/Tyr204) (E10), Cat # CST9106S, 1:1000), Id1 (sc133104,

257 monoclonal, Santa Cruz Biotechnology, 1:100) and an HRP-conjugated secondary antibodies

258 (Cat # ab205719 and ab6721, Abcam, 1:5000). The western blot band densitometric analysis

259 was performed with ImageJ.

260

261 **Precision-cut lung slices (PCLS) culture.** Lung tissue pieces were obtained from a healthy

262 donor collected from the Donor Network West, San Ramon, CA. First, the tissue pieces were

263 inflated with 2% low melting agarose prepared in 1x PBS, and kept on ice for 15mins. Then

264 the solidified pieces were placed onto a petri dish plate and 8mm punch biopsies were

265 carefully made, creating cylinders of lung tissue. 6% agarose was poured into the compress

266 tome mold and the cylinder of lung tissue was quickly placed into the mold, ensuring that 6%

267 agarose surrounded the cylinder on all sides. After being solidified, the tissue pieces were

268 sliced using the compress tome at 400 µm thick slices. The lung slices were then cultured in

269 1x DMEM GlutaMAX medium containing 10% fetal calf serum, penicillin/streptomycin

270 (1%), and amphotericin B (0.1%) in the presence and absence of Brivanib at 10 or 50 µM in

271 1mL of media in a 12-well tissue culture plate. After 24 hrs, the slices were washed with 1x

272 PBS two times and then harvested for RNA isolation.

273

274 **Statistics analysis.** All data analyses were performed using GraphPad Prism V9. All data are

275 represented as the mean $\pm$ standard error of the mean. An unpaired Student's *t*-test was

276 used to compare two groups, and one-way ANOVA was performed for comparing data with

277 more than two groups, followed by an appropriate post-hoc test for multiple comparisons.

278 Brivanib validation data in HHT gene knockdown cells were analysed using two-way

279 repeated measures ANOVA with a Bonferroni post-hoc test. The statistically significant

280 differences were considered at $p < 0.05$.

281

282

283 **Results**

284 **Identifying common downstream gene signatures of HHT-causing genes mutations in**

285 **human PMVECs**

286 As loss of function mutations in ALK1, ENG and SMAD4 are causative of HHT, and as all

287 three genes belong to the TGFβ/BMPR2 super family signaling pathway (**Figure 1A**), we

288 sought to identify common downstream signatures of all three HHT-causing gene mutations

289 in PMVECs by RNAseq following siRNA-mediated silencing of the three genes. We used

290 pulmonary microvascular endothelial cells, PMVECs, as endothelial cells are believed to be

291 the critical cell type for AVM formation, and pulmonary cells, as pulmonary AVMs are one

292 of the most common visceral manifestations in HHT. We first confirmed that following

293 adding BMP ligand, BMP9, BMP signaling is activated in PMVECs, as evidenced by

294 increased pSMAD1/5/9 and Id1 levels measured by western blot (**Figure 1B**). Next, we

295 silenced ALK1, ENG, and SMAD4 with siRNA in PMVECs. As seen in **Figures 1C-E**, we

296 achieved a knockdown of over 80% for all three genes, ALK1, ENG, and SMAD4, measured

297 by qRT-PCR. We activated the pathway with 20ng/mL BMP9 for 2 and 24 hrs in the HHT

298 genes knocked down cells. Stimulation with the ligand BMP9 had no effect on the expression

299 of ALK1, ENG, and SMAD4 (**Figures 1C-E**). We then looked at one of the known

300 downstream targets of the BMPR2/ALK1/ENG/SMAD4 pathway, Id1 (**Figure 1F and G**),

301 and whether the expression of Id1 is reduced by knocking down all three HHT genes.

302 Interestingly, while BMP9-induced Id1 expression is decreased by knocking down ALK1 and

303 SMAD4, a knock-down of ENG did not affect BMP9-induced Id1 expression. In fact, Id1

304 expression was rather slightly increased after ENG knockdown compared to the NT siRNA

305 condition. These findings indicated that Id1 is not a common downstream target of all three

306   HHT genes but is specific for ALK1 and SMAD4 mediated signaling. This is a very

307   important finding when it comes to identifying common downstream targets and

308   subsequently predicting repurposed drugs that might increase the signaling for all three gene

309   mutations.

310

311   Next, we carried out experiments to understand how knocking down ALK1, ENG, and

312   SMAD4 effected the function of PMVECs *in vitro*. We assessed proliferation, apoptosis, and

313   tube formation following the silencing of the three HHT genes with siRNA. The MTT assay

314   showed that knockdown of the HHT genes did not significantly change cell proliferation

315   (**Figure E1A**). Silencing of ENG induced apoptosis as evidenced by increased caspase 3/7

316   activity and decreased angiogenesis, as evidenced by reduced numbers of nodes, junctions

317   and tube length compared to controls at baseline **(Figures E1B and C)**. ALK1 and SMAD4

318   knockdown had no significant effect on apoptosis and tube formation. These results

319   suggested that while ALK1, ENG, and SMAD4 deficiency are linked with HHT, at baseline,

320   only ENG deficiency induced PMVECs dysfunction *in vitro*.

321

322   Since HHT1 and HHT2 patients show similar clinical symptoms, a previous study had

323   identified 277 downregulated and 62 upregulated common downstream targets genes in blood

324   outgrowth endothelial cells isolated from HHT patients carrying ENG (HHT1), ALK1

325   missense or ALK1 non-sense mutations (HHT2) compared to healthy endothelial cells, which

326   they called a "gene expression fingerprinting of HHT"[19]. However, to date, no studies have

327   identified common downstream genes of the three key HHT genes in PMVECs. Thus, we

328   performed RNA sequencing of PMVECs silenced to either ALK1, ENG, or SMAD4 and

329   treated with BMP9 20ng/mL for 2 or 24 hrs. The list of significant differentially expressed

330   genes was identified by employing the criteria of changes in gene expression of log2-fold

331   changes value =>2 and *p* adjusted value =<0.05 between the groups. We identified 117

332   upregulated and 125 downregulated common genes 2hrs after BMP9 stimulation in PMVECs

333   silenced for all three HHT genes (**Figures 2A and C**) and 112 upregulated and 132

334   downregulated common downstream genes 24 hrs after BMP9 stimulation in PMVECs

335   silenced for all three HHT genes (**Figures 2B and C**). Consistent with previously identified

336   genes associated with AVM/HHT[20, 21], we found a significant upregulation of ANGPT2

337   and APLN and downregulation of TMEM100 after 2hrs and 24hrs BMP9 stimulation in

338   PMVECs knockdown cells (KD), respectively, along with other important vascular

339   dysfunction related gene signature changes (**Figures 2A-C**).

340

341   To determine whether the commonly identified downstream targets ("UP and Down genes")
342 of the HHT genes after 2hrs or 24hrs BMP9 stimulation could potentially associate with
343 biological processes and signaling pathways relevant to HHT, we carried out an *in silico*
344 analysis of the common downstream genes using the GO biological process enrichment
345 analysis tool, the DAVID panther pathway analysis tool, and the STRING protein-protein
346 interaction database [22]. GO enrichment analysis of the commonly dysregulated
347 downstream targets uncovered a significant enrichment of HHT-related biological processes,
348 including cell migration, adhesion, tube and vascular development and angiogenesis,
349 extracellular matrix organization, and ion transport after 2 and 24hrs of BMP9 stimulation
350 following HHT gene KD (**Figure 2D**). Moreover, we also observed enrichment of signaling
351 pathways that are thought to regulate AVM formation in HHT, including Wnt signaling,
352 cadherin signaling, integrin signaling, inflammation-mediated cytokines and chemokine
353 signaling, blood coagulation, angiogenesis and TGFβ-signaling pathways (**Figure 2E**).
354 STRING network analysis identified some hub genes, such as PDGFRB, and VCAM that
355 could play roles in AVM/HHT (**Figures E2 A and B**).

356

357   Next, we identified the common persistently and consistently dysregulated gene signatures
358 after 2 and 24 hrs of BMP9 stimulation in the common HHT gene KD conditions. We found
359 5 upregulated genes (Heparan Sulfate-Glucosamine 3-Sulfotransferase 2 (HS3ST2),
360 Glycoprotein Nmb (GPNMB), Ankyrin Repeat Domain 33 (ANKRD33), Ras-related GTP-
361 binding protein D (RRAGD), Lymphatic Vessel Endothelial Hyaluronan Receptor (LYVE1))
362 and 7 downregulated (Carboxypeptidase A4 (CPA4), Solute Carrier Family 25 Member 47
363 (SLC25A47), Shisa Family Member 9 (SHISA9), Histone cluster 1 H2B family member e
364 (HIST1H2BE), Melanocortin 5 Receptor (MC5R), Fibroblast Growth Factor 19 (FGF19),
365 FSHD Region Gene 2 Family Member C (FRG2C)) genes (**Figure 3A**). qRT-PCR validation
366 of the common persistently dysregulated genes in PMVECs further confirmed upregulation
367 of GPNMB and LYVE1 and downregulation of MC5R in the common HHT KD conditions
368 after BMP9 stimulation. As further validation, those genes were regulated in the opposite
369 direction when stimulated with BMP9 alone (**Figures 3B and C and Figures E3 A-D**). We
370 therefore concentrated on MC5R, GPNMB, and LYVE1 to investigate further their known
371 importance related to HHT. LYVE1 expression was positively correlated with preoperative
372 edema in brain AVM [23], while the role of MC5R and GPNMB in AVM formation and

373 HHT is unknown. Our in vitro functional assays did not exhibit significant changes in cell
374 proliferation, apoptosis, and tube formation in PMVECs silenced to either MC5R, GPNMB
375 or LYVE1 at baseline (**Figures E3 E-G**).
376

377 **In silico screening of drugs that can reverse common downstream gene signatures of**
378 **HHT causing gene mutations**
379 We hypothesized that novel/re-purposed drugs could reverse the HHT/PAVM pathological
380 downstream targets/signaling and thereby reverse abnormal endothelial cell functions (tube
381 formation, migration, proliferation) in PMVECs. A powerful strategy to predict novel drugs
382 that might be beneficial in HHT is to use bioinformatics approaches to match in silico drug
383 gene expression profiles with disease or anti-disease signature profiles, as previously shown
384 by our group [8]. Here, we used the list of commonly upregulated genes that were
385 differentially expressed in PMVEC silenced to all three HHT genes and stimulated with
386 BMP9 for 2 and 24hrs, 117 and 112, respectively, which we labelled as "HHT disease
387 signature". This transcriptomic gene expression signature served as blueprint for predicting
388 potentially beneficial drugs that mimic the complementary "anti-signature" using the Broad
389 Institute's Clue.io query app https://clue.io/query. We uploaded the genes on the web-based
390 application database and selected with the gene expression L1000 query parameter. This
391 web-based clue query app allows queries with external gene sets to identify compounds that
392 either mimic our gene sets' transcriptional signatures or reverse the signature (anti-signatures)
393 in different cell lines. We narrowed down the drug list based on the findings from the
394 HUVECs data sets as this is the closest cell line to our data sets acquired in PMVECs. The
395 drugs were ranked following the criteria of samples >=3, tas values >=0.20, normalized
396 connectivity score, and FDR values on the query app. Top scoring 5 HHT and anti-HHT
397 drugs are shown in **Figure 4B**. From the top anti-HHT drug candidates (negative values)
398 (24h), we concentrated on Brivanib as it is well-known for its anti-FGF/VEGF activities [24].
399 We hypothesized that Brivanib would on the one hand, reverse the dysfunctional downstream
400 targets related to BMP signaling and on the other hand could inhibit the overactivated VEGF
401 pathway in HHT. To test the effect Brivanib had on restoring members of dysfunctional BMP
402 signaling, we determined whether Brivanib reversed the 5 upregulated (LYVE1, GPNMB,
403 RRAGD, ANKRD33, HS3ST2) and 7 downregulated (MC5R, SLC25A47, FGF19, SHISA9,
404 FRG2C, HIST1H2BE, CPA4) genes, we had previously defined a being consistently
405 dysregulated after silencing of all three HHT genes and stimulation with BMP9 for 2 and
406 24hrs. Importantly, we observed that Brivanib inhibited the expression of LYVE1, GPNMB,

12

407 RRAGD, and ANKRD33 induced in HHT gene KD conditions (**Figures 4C-F and E4 A-C**).

408 Furthermore, Brivanib rescued the expression of the MC5R, SLC25A47, FGF19, SHISA9,

409 and FRG2C that were downregulated in HHT gene KD conditions (**Figures 4G-K and E4 A-**

410 **C**). These results demonstrated that Brivanib could improve the dysfunctional

411 ALK1/ENG/SMAD4 signaling in HHT.

412

413 **Brivanib inhibited the commonly upregulated downstream gene expression signatures**

414 **of HHT-causing genes in ex vivo PCLS**

415 To investigate whether Brivanib also inhibited the commonly upregulated signatures of HHT-

416 causing genes in human lung tissue, we measured expression of LYVE1, GPNMB, HS3ST2,

417 RRAGD, and ANKRD33 using qRT-PCR in human PCLS treated with Brivanib for 24 hrs.

418 PCLS were prepared from a healthy human donor obtained from Donor Network West,

419 California. PCLS were treated with 50 uM Brivanib or DMSO for 24 hrs and then harvested

420 for RNA isolation (**Figure 5A**). Brivanib inhibited mRNA expression of LYVE1, GPNMB,

421 and HS3ST2 in PCLS (**Figures 5B-F**). This inhibition in GPNMB, LYVE1and HS3ST2

422 expression *ex vivo* was similar to the inhibition of those genes in PMVECs after HHT gene

423 knockout and Brivanib treatment *in vitro*. Brivanib did not change expression of RRAGD and

424 ANKRD33 in PCLS.

425

426 **Brivanib inhibited VEGF-induced ERK1/2 MAPK, -VEGF-induced PMVECs**

427 **proliferation and tube formation *in vitro***

428 As over-activation of pro-angiogenic pathways, such as VEGF signaling, is strongly linked

429 with the development of vascular dysfunction in HHT, and as Brivanib was previously shown

430 to exhibit anti-VEGF effects both *in vitro* and *in vivo* in cancer and liver fibrosis studies [24-

431 26], we carried out cell culture experiments to determine whether Brivanib can also inhibit

432 the VEGF signaling pathway in PMVECs. PMVECs were cultured in the presence and

433 absence of 10 μM Brivanib or DMSO in serum starvation media (0.2% FCS) for 24 hrs and

434 then stimulated with 40 ng/mL VEGF for 10 mins. We measured phospho-ERK1/2 MAPK,

435 total ERK1/2 MAPK (a downstream target of VEGF signaling) levels by western blotting.

436 Notably, our results showed that Brivanib completely blocked VEGF-induced phospho-

437 ERK1/2 levels in PMVECs (**Figure 6A**).

438

439 We next assessed functional properties and endothelial behaviors with regards to tube

440 formation and proliferation with and without Brivanib treatment. To determine whether

441   Brivanib inhibits the VEGF-induced proliferation of PMVECs, we performed an MTT assay

442   to measure the viability of PMVECs treated with VEGF (20 ng/mL) in the presence and

443   absence of Brivanib (10 µM) in serum-starved media (0.2% FCS). As expected, VEGF

444   treatment significantly increased PMVECs proliferation (**Figure 6B**). Importantly, Brivanib

445   completely blocked the VEGF-induced proliferation of PMVECs (**Figure 6B**). Brivanib

446   alone, without ligand stimulation, did not change proliferation of PMVECs. These findings

447   suggested that Brivanib attenuated VEGF-induced PMVECs proliferation *in vitro*. To further

448   explore the anti-angiogenic role of Brivanib on PMVECs *in vitro*, a matrigel based tube

449   formation assay was performed. Results revealed that Brivanib inhibited tube formation in

450   PMVECs as evidenced by the decreased number of junctions and total tube lengths compared

451   to DMSO-treated control cells (**Figure 6C**).

452

453   **Discussion**

454   In this study, we identified common downstream targets/pathways of the three HHT-causing

455   genes, ALK1, ENG, and SMAD4 using whole genome RNAseq following knock down of the

456   HHT genes in PMVECs *in vitro*. We also investigated whether we could identify a drug that

457   can reverse the dysregulated downstream gene signatures and improve the common

458   downstream dysfunctional pathways and HHT-related dysfunction of cellular phenotypes.

459   Here, we found that ID1, a major downstream target of the TGFß/BMP signaling pathway, is

460   not a common downstream target of all the HHT gene knockdown (ALK1, ENG, or SMAD4)

461   conditions, while other downstream targets, such as LYVE1, GPNMB, PLXDC2, and MC5R,

462   are downstream of all three HHT genes. Furthermore, we identified a small molecule drug,

463   Brivanib, that could, on the one hand, reverse the downstream gene signatures following

464   knockdown of all three HHT genes and, on the other hand, inhibit the VEGF signaling

465   pathway, improve proliferation and tube formation in PMVECs. These findings suggest that

466   Brivanib might be effective in treating AVMs and HHT by normalizing dysfunctional

467   downstream signaling.

468

469   ID1 has been used as a downstream readout of BMPR2 signaling, and increasing ID1 as a

470   therapeutic approach has been shown to be effective in PAH [8, 10]. HHT and PAH are both

471   related rare genetic diseases, characterized by haploinsuffiency in members of the

472   TGFß/BMPR2 signaling pathway. Mutations in BMPR2 cause PAH in up to 20% of patients,

473   whereas mutations in ALK1, ENG and SMAD4 cause HHT in over 85% of patients.

474   Furthermore, there is an overlap between both diseases, as up to up to 10% of HHT patients
475   show elevated pulmonary arterial pressures that indicate either the presence of Group 1 PAH
476   (1% of HHT patients) or Group 2 PH associated with high output failure due to liver AVMs
477   (more common, 10%) [27, 28].Our group previously discovered BMPR2 signaling inhibitors
478   FHIT [8] and LCK [18], and BMPR2 signaling activating drugs FK506 [9] and Enzastaurin
479   [8] by performing a high throughput screen (HTS) of siRNAs as well as FDA approved drugs
480   to identify modifier genes and drugs that activate the BMPR2 pathway. Both screens were
481   performed using the myoblastoma reporter cell line in which the BMP response element
482   (BRE) from the ID1 promotor was linked to Luciferase (BRE-Luc). The BMPR2 signaling
483   downstream target ID1 was the readout to measure activation of BMPR2 signaling in these
484   HTS. As BMPR2 is the co-receptor of ALK1/ENG signaling we therefore first determined
485   whether ID1 could be used as a common readout in HHT as well. We found that ID1
486   expression was not decreased by ENG knockdown, in contrast to ALK1 or SMAD4
487   knockdown, which inhibited BMP9 induced ID1 expression in PMVECs. While being a valid
488   readout for ALK1 and SMAD4 mediated signaling, ID1 was not a readout for ENG signaling.
489   In order to predict drugs that would normalize downstream signaling of all three HHT genes,
490   we had to identify novel common downstream targets.
491
492   We used siRNA mediated, >80% knockdown of ENG, ALK1 or SMAD4 in PMVECs to
493   mimic the proposed complete loss-of function of the above genes in endothelial cells of
494   AVMs *in vivo*. While germline mutations in ALK1, ENG, or SMAD4 lead to
495   haploinsufficiency and are required for AVM formation, several studies have suggested that
496   they are not sufficient and that additional genetic and environmental factors are required to
497   generate AVMs [29]. As an example, in order to establish skin and brain AVMs in adult mice
498   lacking ALK1, the creation of a wound or stimulation with VEGF, two angiogenic triggers,
499   were required for AVM formation [30-33]. It is proposed that these triggers might lead to a
500   complete loss of function and signaling downstream of the HHT genes. This concept is
501   further supported by the recent identification of somatic mutations in addition to germline
502   mutations in endothelial cells of AVM lesions resulting in a bi-allelic loss of ENG or
503   ALK1[15]. While the siRNA mediated complete loss of ENG, ALK1 or SMAD4 in PMVECs
504   therefore mimics the *in vivo* loss of function, silencing of ENG, ALK1 or SMAD4 had no
505   effect on PMVEC proliferation. Of interest ENG silencing decreased angiogenesis and
506   induced apoptosis in PMVECs at baseline. Therefore the *in vitro* phenotype, without the use

507   of additional stimuli such as VEGF (**Figure 6**) is not an adequate surrogate for the

508   endothelial behavior after HHT KD in *vivo*.

509

510   To determine the common downstream targets of HHT-causing genes, we profiled gene

511   expression by RNAseq following silencing of either ALK1, ENG, or SMAD4 in PMVECs.

512   Our RNAseq analysis revealed, in addition to novel common downstream targets, several

513   genes, such as ANGPT2, APLN, and TMEM100 (**Figure 2C**) that have previously been

514   reported to be involved in AVM formation and HHT pathogenesis [20, 21]. This indicates

515   that the list of common downstream genes could mimic AVM and HHT gene signatures.

516   Angpt2 encodes for angiopoietin 2, an antagonistic ligand for TEK (TEK receptor tyrosine

517   kinase, an EC surface receptor). Through RNAseq analysis Crist et al. found that Angpt2 was

518   upregulated whereas Tek levels were downregulated in ECs isolated from the retina of

519   *Smad4*-iECKO mice, a hereditary HHT mouse model. EC-specific Smad4 knockout resulted

520   in an increase in Angpt2 transcription in those ECs that caused AVM formation in the retina

521   [20]. Targeting Angpt2 with anti-ANGPT2 antibodies (LC-10) was shown to protect and

522   rescue AVM formation of *Smad4*-iECKO mice, further supporting the role of ANGPT2 as a

523   crucial TGFβ-downstream mediator of AVM development in the retina [20]. The same

524   research team also found an upregulation of Apln (Apelin) in isolated lung ECs and retinas of

525   *Smad4*-iECKO mice [34]. Apln is a ligand for the APJ receptor (also known as APLNR)

526   which is a G-protein-coupled receptor. Previous studies showed a significant reduction of

527   ECs proliferation and vascular outgrowth, abnormal arterial-venous alignment, and narrow

528   blood vessels of mice and frog embryos deficient in either APLN or APLNR [35-41].

529   Hypoxia-induced APLN expression, and exogenous apelin treatment increased proliferation,

530   migration, and inhibited apoptosis in mouse brain ECs *in vitro* [35]. APLN mRNA

531   expression was also found to be downregulated by BMP signaling in human dermal

532   microvascular ECs, and the BMP-APLN/APLNR signaling axis was crucial for hypoxia-

533   induced ECs growth [42]. The APLN/APLNR pathway plays a significant role in various

534   diseases, including pulmonary hypertension, and there is a strong relationship between BMP

535   and APLN/APLNR in vascular signaling. However, the causal involvement of

536   APLN/APLNR in AVM and HHT remains to be investigated. TMEM100 (encodes

537   transmembrane protein 100) been shown to be enriched in arterial endothelium and activated

538   by the BMP9/BMP10/ALK1 signaling axis [21, 43]. Intriguingly, mice lacking TMEM100

539   show substantial arterial specific abnormalities, embryonic lethality, and AVM formations,

540   similar phenotypes seen in Alk1 constitutive KO mice [43, 44], suggesting that TMEM100

541   plays a significant role for arterial endothelium differentiation and vascular morphogenesis.
542   Although Moon et al., claimed that TMEM100 is necessary for maintaining vascular integrity
543   and angiogenesis, even though it is not the primary mechanism behind HHT pathogenesis,
544   TMEM deficiency may contribute to the onset of HHT by weakening vascular integrity [21].
545   While there are no studies available that identify gene expression profiles of the HHT genes
546   in PMVECs, three studies profiled genes expression in BOECs [19], HUVECs [45] and nasal
547   telangiectasia tissue [46] of HHT patients. We compared our common gene list with the
548   reported gene expression list of BOECs from HHT1 and HHT2 patients and found that 15
549   gene that were described to be dysregulated were common with our data set (PRCP,
550   SLC40A1, MYO5C KCNH4, MGP, CPA4, MMP1, ANGPT2, ENG, APLN, HHIP, FABP4,
551   AKR1C3, IGFBP3, and ESM1) [19]. Interestingly, among the 15 dysregulated genes, we
552   only ENG and ESM1 (endothelial cell specific molecule 1) were changed in the same
553   direction (upregulation) in the HHT BOECs when compared to our dataset. However MGP,
554   MMP1, and TNFRS4 were upregulated and COL3A1 was downregulated in HUVECs of
555   HHT1 and HHT2 patients as well as in our dataset [45]. The differences in altered gene
556   expression profiles between our studies and the above-mentioned gene expression profiling
557   studies could be explained by the fact that the authors used BOECs derived from HHT
558   patients, which potentially were only haplo-insufficient for the specific gene mutation,
559   whereas we used HHT gene-deficient PMVECs (80% knockdown). Together these findings
560   suggest that the common downstream targets of the completely silenced HHT genes, we
561   identified through RNAseq could potentially serve as a common HHT disease gene signature.
562

563   Furthermore, the top biological processes of the list of the common genes were significantly
564   enriched for angiogenesis, blood vessels morphogenesis and development, vasculature
565   development, tube morphogenesis and development, cell adhesion and migration, organ
566   morphogenesis and development, regulation of signal transductions, and ECM organization
567   (**Figure 2D**), all processes that are relevant to AVM formation and HHT pathogenesis [47].
568   The top signaling pathways enriched by the common genes list include Wnt, Cadherin,
569   Integrin, TGFβ, chemokines and cytokines mediated inflammatory and angiogenesis
570   pathways. While the involvement of TGFβ, inflammatory mediated signaling and angiogenic
571   pathways in HHT is already known, the role of the Wnt signaling pathway in HHT still needs
572   to be explored.
573

574   Next, by comparing two conditions, 2 and 24 hrs after BMP9 stimulation following silencing
575   of the three HHT genes, we identified commonly altered gene signatures that were
576   persistently dysregulated, LYVE1, GPNMB, MC5R and PLXDC2. We narrowed down the
577   list of common persistent gene signatures by choosing those genes that showed an opposite
578   direction of gene expression when stimulated with BMP9 for 2h and 24hrs versus when
579   stimulated after complete gene knockdown. LYVE1 is expressed in lymphatic ECs but is also
580   in developing blood vessels and macrophages. A previous study found increased expression
581   of LYVE1 in human brain AVMs and the expression of LYVE1 was found to be positively
582   associated with preoperative edema [23]. Glycoprotein non-metastatic melanoma protein B
583   (GPNMB), a transmembrane protein, was shown to be linked with increased endothelial
584   recruitment in a breast cancer study [48]. The activation of melanocortin receptors (MC1R
585   and MC5R) in a mouse model of diabetic retinopathy improved retinal damage, prevented
586   changes to the blood retinal barrier, and reduced local pro-inflammatory and pro-angiogenic
587   factors, such as cytokines, chemokines, and VEGF [49]. PLXDC2, also known as tumor
588   endothelial marker 7-related protein, TEM7R, is highly expressed in breast cancer and colon
589   cancer tissues [50, 51]. These studies suggest that LYVE1, GPNMB, MC5R and PLXDC2
590   might play an important role in endothelial and vascular homeostasis in health and disease.
591   Further studies are needed to confirm their causative role in AVM formation and HHT.
592
593   Currently, treatment options for HHT are limited. Several promising HHT drugs have been
594   tested in clinical and preclinical settings. Bevacizumab (Avastin, anti-VEGF monoclonal
595   antibody) [14, 52], Tacrolimus (FK506, a BMP signaling activator) [12, 53, 54], Pazopanib
596   (TKI) [55], and Thalidomide (increases expression of PDGFB) [56] all have been shown to
597   decrease epistaxis in HHT patients. In the genetically induced animal models of HHT, several
598   drugs, such as Wortmannin, Pictilisib (a PI3K inhibitor) [57, 58], DC101 (an anti-VEGFR2
599   antibody)[59], SU5416 (a VEGFR2 inhibitor)[58], LC10 (a ANGPT2 inhibitor)[20], and
600   G6.31 (a anti-VEGFA antibody) [32] have been shown to prevent or reduce retinal,
601   peripheral or skin AVMs in neonate or adult mice. Recently, correcting multiple signaling
602   pathways associated with AVM/HHT simultaneously, such as SMAD1/5/9, VEGFR2, and
603   AKT/PI3K with combined treatment of drugs that target the above signaling (Sirolimus and
604   Nintedanib) has also been shown to be effective in reducing and reversing retinal AVMs in
605   the anti-BMP9/10 monoclonal antibody-induced HHT model in neonate and adult mice.
606   While these drugs show promising findings in preclinical and clinical studies, several
607   obstacles need to be addresses before a successful translation into the clinic can be made. As

608   an example, FK506, an immunosuppressive drug, was demonstrated to improve vascular
609   pathology in animal models [13], yet had minimal effects on epistaxis in a RCT HHT clinical
610   trial when used as a topical ointment[53], while demonstration some efficacy yet also adverse
611   effects when taken orally[54]. Further larger clinical studies are needed to confirm these
612   findings. Furthermore, FK506 was discovered using ID1 as readout in the mouse
613   myoblastoma BRE-Luc reporter cell line. As we found that ID1 is a common downstream
614   target of ALK1 and SMAD4, but not necessarily ENG, this would suggest that FK506 may
615   not be the optimal treatment for ENG-mutant HHT patients. In addition, while several
616   clinical and animal studies document that anti-VEGF antibodies or VEGF inhibitors are
617   effective to reduce bleeding events and anemia, the VEGF/VEGFR2 signaling pathway is
618   complex and involves many downstream signaling pathway[60]. It is unclear which pathway
619   (or combination of pathways) needs to be targeted precisely to facilitate regression of AVMs.
620   Moreover, the understanding of the crosstalk between VEGF and BMP signaling is still
621   limited, and how the two signaling pathways are disrupted in HHT is not completely known.
622
623   Our strategy to identify beneficial drugs for HHT is different from previous approaches. We
624   predicted drugs based on their ability to reverse common downstream targets of HHT-causing
625   genes and narrowed down the top candidates by introducing a second selection criterium: the
626   drug should have in addition anti-VEGF properties. Using this approach, we selected three
627   top-scoring potential HHT drugs (Brivanib, Cediranib, and Glesatinib). Among these drugs,
628   we found that Brivanib can improve the dysfunctional common downstream gene signatures
629   in PMVECs subjected to silencing of either ALK1, ENG or SMAD4 or in the *ex vivo* PCLS
630   system. Brivanib also reversed VEGF-induced downstream signaling pathways and improved
631   endothelial function *in vitro*. Although our findings all stem from *in vitro* or *ex vivo* studies,
632   in the context of the drug discovery based on signaling pathways, our findings are
633   comparable to the findings of a previously reported study in which the authors used a
634   combined drug treatment to correct SMAD1/5/9, VEGF and mTOR signaling. We, on the
635   other hand, identified Brivanib which was capable of correcting the downstream HHT as well
636   as VEGF signaling simultaneously. Brivanib is a well-known VEGF signaling inhibitor [25,
637   61-63]. Our study suggests that Brivanib could be effective in HHT by correcting
638   downstream targets of HHT causing gene signatures as well as VEGF signaling to positively
639   influence AVM formation and growth (**Figure 6D**).
640

641   In summary, the present study used a RNAseq high throughput approach following loss of
642   function mutations of the HHT causing genes to identify the common downstream gene
643   signatures. Drugs were predicted based on their capability to mimic downstream HHT gene
644   signatures as well as their anti-VEGF properties. Our findings suggest that ID1 is not a
645   common downstream target of ENG but is specific for ALK1 and SMAD4 in PMVECs. We
646   also revealed that Brivanib is superior to the use of a VEGF inhibition alone, as it restores
647   normal HHT downstream signaling and thereby could be tested to prevent, halt or reverse
648   AVMs. As all our findings of Brivanib are based on *in vitro* and *ex vivo* studies, Brivanib
649   would need to be tested in *in vivo* HHT animal models and in clinical studies to further
650   confirm these findings.

651

652

653   **Support statement**

657

658   **Author contributions**

659   Conceptualization: M.K.A., E.S.; Methodology: M.K.A; Data curation: M.K.A., Y.L., N.H.J.,
660   C.A.S., Z., M.; Writing - original draft: M.K.A.; Writing - review & editing: M.K.A., E.S.,
661   K.S.; Supervision: E.S., Funding acquisition: E.S.

662

663   **Acknowledgement**

667

668   **Conflict of Interest statement:**

669   The authors declare no competing or financial interests.

670   A patent application for the use of Brivanib in HHT is currently filed by Stanford University.

671

672   **References**

673   1.   Schimmel, K., et al., *Arteriovenous Malformations-Current Understanding of the*
674   *Pathogenesis with Implications for Treatment.* Int J Mol Sci, 2021. **22**(16).

675   2.   Angel, C.M., *Hereditary Hemorrhagic Telangiectasia: Diagnosis and Management.* J
676   Clin Med, 2022. **11**(16).

677   3.   Shovlin, C.L., et al., *Diagnostic criteria for hereditary hemorrhagic telangiectasia*
678   *(Rendu-Osler-Weber syndrome).* Am J Med Genet, 2000. **91**(1): p. 66-7.

679   4.   Robert, F., et al., *Future treatments for hereditary hemorrhagic telangiectasia.*
680   Orphanet J Rare Dis, 2020. **15**(1): p. 4.

681   5.   Ruiz, S., et al., *Correcting Smad1/5/8, mTOR, and VEGFR2 treats pathology in*
682   *hereditary hemorrhagic telangiectasia models.* J Clin Invest, 2020. **130**(2): p. 942-
683   957.

684   6.   Goumans, M.J., et al., *Bone Morphogenetic Proteins in Vascular Homeostasis and*
685   *Disease.* Cold Spring Harb Perspect Biol, 2018. **10**(2).

686   7.   Lyden, D., et al., *Id1 and Id3 are required for neurogenesis, angiogenesis and*
687   *vascularization of tumour xenografts.* Nature, 1999. **401**(6754): p. 670-7.

688   8.   Dannewitz Prosseda, S., et al., *FHIT, a Novel Modifier Gene in Pulmonary Arterial*
689   *Hypertension.* Am J Respir Crit Care Med, 2019. **199**(1): p. 83-98.

690   9.   Spiekerkoetter, E., et al., *FK506 activates BMPR2, rescues endothelial dysfunction,*
691   *and reverses pulmonary hypertension.* J Clin Invest, 2013. **123**(8): p. 3600-13.

692   10.   Spiekerkoetter, E., et al., *Randomised placebo-controlled safety and tolerability trial*
693   *of FK506 (tacrolimus) for pulmonary arterial hypertension.* Eur Respir J, 2017. **50**(3).

694   11.   Spiekerkoetter, E., et al., *Low-Dose FK506 (Tacrolimus) in End-Stage Pulmonary*
695   *Arterial Hypertension.* Am J Respir Crit Care Med, 2015. **192**(2): p. 254-7.

696   12.   Sommer, N., et al., *Treatment with low-dose tacrolimus inhibits bleeding*
697   *complications in a patient with hereditary hemorrhagic telangiectasia and pulmonary*
698   *arterial hypertension.* Pulm Circ, 2019. **9**(2): p. 2045894018805406.

699   13.   Ruiz, S., et al., *Tacrolimus rescues the signaling and gene expression signature of*
700   *endothelial ALK1 loss-of-function and improves HHT vascular pathology.* Hum Mol
701   Genet, 2017. **26**(24): p. 4786-4798.

702   14.   Al-Samkari, H., et al., *An international, multicenter study of intravenous bevacizumab*
703   *for bleeding in hereditary hemorrhagic telangiectasia: the InHIBIT-Bleed study.*
704   Haematologica, 2021. **106**(8): p. 2161-2169.

705   15.   Snellings, D.A., et al., *Somatic Mutations in Vascular Malformations of Hereditary*
706   *Hemorrhagic Telangiectasia Result in Bi-allelic Loss of ENG or ACVRL1.* Am J Hum
707   Genet, 2019. **105**(5): p. 894-906.

708   16.   Tual-Chalot, S., S.P. Oh, and H.M. Arthur, *Mouse models of hereditary hemorrhagic*
709   *telangiectasia: recent advances and future challenges.* Front Genet, 2015. **6**: p. 25.

710   17.   Ali, M.K., et al., *Crucial role for lung iron level and regulation in the pathogenesis*
711   *and severity of asthma.* Eur Respir J, 2020. **55**(4).

712   18.   Andruska, A.M., et al., *Selective Src-Family B Kinase Inhibition Promotes Pulmonary*
713   *Artery Endothelial Cell Dysfunction.* bioRxiv, 2021: p. 2021.09.27.462034.

714   19.   Fernandez, L.A., et al., *Gene expression fingerprinting for human hereditary*
715   *hemorrhagic telangiectasia.* Hum Mol Genet, 2007. **16**(13): p. 1515-33.

716   20.   Crist, A.M., et al., *Angiopoietin-2 Inhibition Rescues Arteriovenous Malformation in*
717   *a Smad4 Hereditary Hemorrhagic Telangiectasia Mouse Model.* Circulation, 2019.
718   **139**(17): p. 2049-2063.

719   21.   Moon, E.H., et al., *Essential role for TMEM100 in vascular integrity but limited*
720   *contributions to the pathogenesis of hereditary haemorrhagic telangiectasia.*
721   Cardiovasc Res, 2015. **105**(3): p. 353-60.

722   22.   Szklarczyk, D., et al., *STRING v11: protein-protein association networks with*
723   *increased coverage, supporting functional discovery in genome-wide experimental*
724   *datasets.* Nucleic Acids Res, 2019. **47**(D1): p. D607-D613.

725   23.   Shoemaker, L.D., et al., *Human brain arteriovenous malformations express*
726   *lymphatic-associated genes.* Ann Clin Transl Neurol, 2014. **1**(12): p. 982-95.

727   24.   Dempke, W.C. and R. Zippel, *Brivanib, a novel dual VEGF-R2/bFGF-R inhibitor.*
728   Anticancer Res, 2010. **30**(11): p. 4477-83.

729   25.   Nakamura, I., et al., *Brivanib attenuates hepatic fibrosis in vivo and stellate cell*
730   *activation in vitro by inhibition of FGF, VEGF and PDGF signaling.* PLoS One,
731   2014. **9**(4): p. e92273.

732   26.   Huynh, H., et al., *Brivanib alaninate, a dual inhibitor of vascular endothelial growth*
733   *factor receptor and fibroblast growth factor receptor tyrosine kinases, induces growth*
734   *inhibition in mouse models of human hepatocellular carcinoma.* Clin Cancer Res,
735   2008. **14**(19): p. 6146-53.

736   27.   Abston, E., et al., *Treatment of pulmonary hypertension in patients with Hereditary*
737   *Hemorrhagic Telangiectasia - A case series and systematic review.* Pulm Pharmacol
738   Ther, 2021. **68**: p. 102033.

739   28.   Vorselaars, V., et al., *Pulmonary Hypertension in a Large Cohort with Hereditary*
740   *Hemorrhagic Telangiectasia.* Respiration, 2017. **94**(3): p. 242-250.

741   29.   Bernabeu, C., et al., *Potential Second-Hits in Hereditary Hemorrhagic*
742   *Telangiectasia.* J Clin Med, 2020. **9**(11).

743   30.   Park, S.O., et al., *Real-time imaging of de novo arteriovenous malformation in a*
744   *mouse model of hereditary hemorrhagic telangiectasia.* J Clin Invest, 2009. **119**(11):
745   p. 3487-96.

746   31.   Garrido-Martin, E.M., et al., *Common and distinctive pathogenetic features of*
747   *arteriovenous malformations in hereditary hemorrhagic telangiectasia 1 and*
748   *hereditary hemorrhagic telangiectasia 2 animal models--brief report.* Arterioscler
749   Thromb Vasc Biol, 2014. **34**(10): p. 2232-6.

750   32.   Han, C., et al., *VEGF neutralization can prevent and normalize arteriovenous*
751   *malformations in an animal model for hereditary hemorrhagic telangiectasia 2.*
752   Angiogenesis, 2014. **17**(4): p. 823-830.

753   33.   Walker, E.J., et al., *Arteriovenous malformation in the adult mouse brain resembling*
754   *the human disease.* Ann Neurol, 2011. **69**(6): p. 954-62.

755   34.   Crist, A.M., et al., *Vascular deficiency of Smad4 causes arteriovenous malformations:*
756   *a mouse model of Hereditary Hemorrhagic Telangiectasia.* Angiogenesis, 2018.
757   **21**(2): p. 363-380.

758   35.   Cox, C.M., et al., *Apelin, the ligand for the endothelial G-protein-coupled receptor,*
759   *APJ, is a potent angiogenic factor required for normal vascular development of the*
760   *frog embryo.* Dev Biol, 2006. **296**(1): p. 177-89.

761   36.   Kalin, R.E., et al., *Paracrine and autocrine mechanisms of apelin signaling govern*
762   *embryonic and tumor angiogenesis.* Dev Biol, 2007. **305**(2): p. 599-614.

763   37.   Papangeli, I., et al., *MicroRNA 139-5p coordinates APLNR-CXCR4 crosstalk during*
764   *vascular maturation.* Nat Commun, 2016. **7**: p. 11268.

765   38.   Kidoya, H., et al., *Spatial and temporal role of the apelin/APJ system in the caliber*
766   *size regulation of blood vessels during angiogenesis.* EMBO J, 2008. **27**(3): p. 522-
767   34.

768   39.   del Toro, R., et al., *Identification and functional analysis of endothelial tip cell-*
769   *enriched genes.* Blood, 2010. **116**(19): p. 4025-33.

770   40.   Kidoya, H., H. Naito, and N. Takakura, *Apelin induces enlarged and nonleaky blood*
771   *vessels for functional recovery from ischemia.* Blood, 2010. **115**(15): p. 3166-74.

772   41.   Kidoya, H., et al., *APJ Regulates Parallel Alignment of Arteries and Veins in the Skin.*
773   Dev Cell, 2015. **33**(3): p. 247-59.

774   42. Poirier, O., et al., *Inhibition of apelin expression by BMP signaling in endothelial*
775   *cells.* Am J Physiol Cell Physiol, 2012. **303**(11): p. C1139-45.

776   43. Somekawa, S., et al., *Tmem100, an ALK1 receptor signaling-dependent gene essential*
777   *for arterial endothelium differentiation and vascular morphogenesis.* Proc Natl Acad
778   Sci U S A, 2012. **109**(30): p. 12064-9.

779   44. Urness, L.D., L.K. Sorensen, and D.Y. Li, *Arteriovenous malformations in mice*
780   *lacking activin receptor-like kinase-1.* Nat Genet, 2000. **26**(3): p. 328-31.

781   45. Thomas, B., et al., *Altered endothelial gene expression associated with hereditary*
782   *haemorrhagic telangiectasia.* Eur J Clin Invest, 2007. **37**(7): p. 580-8.

783   46. Torring, P.M., et al., *Global gene expression profiling of telangiectasial tissue from*
784   *patients with hereditary hemorrhagic telangiectasia.* Microvasc Res, 2015. **99**: p.
785   118-26.

786   47. Locke, T., J. Gollamudi, and P. Chen, *Hereditary Hemorrhagic Telangiectasia*
787   *(HHT)*, in *StatPearls*. 2022: Treasure Island (FL).

788   48. Rose, A.A., et al., *ADAM10 releases a soluble form of the GPNMB/Osteoactivin*
789   *extracellular domain with angiogenic properties.* PLoS One, 2010. **5**(8): p. e12093.

790   49. Gesualdo, C., et al., *Fingolimod and Diabetic Retinopathy: A Drug Repurposing*
791   *Study.* Front Pharmacol, 2021. **12**: p. 718902.

792   50. Rmali, K.A., M.C. Puntis, and W.G. Jiang, *Prognostic values of tumor endothelial*
793   *markers in patients with colorectal cancer.* World J Gastroenterol, 2005. **11**(9): p.
794   1283-6.

795   51. Davies, G., et al., *Levels of expression of endothelial markers specific to tumour-*
796   *associated endothelial cells and their correlation with prognosis in patients with*
797   *breast cancer.* Clin Exp Metastasis, 2004. **21**(1): p. 31-7.

798   52. Dupuis-Girod, S., et al., *Bevacizumab in patients with hereditary hemorrhagic*
799   *telangiectasia and severe hepatic vascular malformations and high cardiac output.*
800   JAMA, 2012. **307**(9): p. 948-55.

801   53. Dupuis-Girod, S., et al., *Efficacy and Safety of a 0.1% Tacrolimus Nasal Ointment as*
802   *a Treatment for Epistaxis in Hereditary Hemorrhagic Telangiectasia: A Double-*
803   *Blind, Randomized, Placebo-Controlled, Multicenter Trial.* J Clin Med, 2020. **9**(5).

804   54. Hessels, J., et al., *Efficacy and Safety of Tacrolimus as Treatment for Bleeding*
805   *Caused by Hereditary Hemorrhagic Telangiectasia: An Open-Label, Pilot Study.* J
806   Clin Med, 2022. **11**(18).

807   55.   Faughnan, M.E., et al., *Pazopanib may reduce bleeding in hereditary hemorrhagic*
808   *telangiectasia.* Angiogenesis, 2019. **22**(1): p. 145-155.
809   56.   Lebrin, F., et al., *Thalidomide stimulates vessel maturation and reduces epistaxis in*
810   *individuals with hereditary hemorrhagic telangiectasia.* Nat Med, 2010. **16**(4): p.
811   420-8.
812   57.   Ola, R., et al., *PI3 kinase inhibition improves vascular malformations in mouse*
813   *models of hereditary haemorrhagic telangiectasia.* Nat Commun, 2016. **7**: p. 13650.
814   58.   Jin, Y., et al., *Endoglin prevents vascular malformation by regulating flow-induced*
815   *cell migration and specification through VEGFR2 signalling.* Nat Cell Biol, 2017.
816   **19**(6): p. 639-652.
817   59.   Tual-Chalot, S., et al., *Loss of Endothelial Endoglin Promotes High-Output Heart*
818   *Failure Through Peripheral Arteriovenous Shunting Driven by VEGF Signaling.* Circ
819   Res, 2020. **126**(2): p. 243-257.
820   60.   Abhinand, C.S., et al., *VEGF-A/VEGFR2 signaling network in endothelial cells*
821   *relevant to angiogenesis.* J Cell Commun Signal, 2016. **10**(4): p. 347-354.
822   61.   Allen, E., I.B. Walters, and D. Hanahan, *Brivanib, a dual FGF/VEGF inhibitor, is*
823   *active both first and second line against mouse pancreatic neuroendocrine tumors*
824   *developing adaptive/evasive resistance to VEGF inhibition.* Clin Cancer Res, 2011.
825   **17**(16): p. 5299-310.
826   62.   Bhide, R.S., et al., *The antiangiogenic activity in xenograft models of brivanib, a dual*
827   *inhibitor of vascular endothelial growth factor receptor-2 and fibroblast growth*
828   *factor receptor-1 kinases.* Mol Cancer Ther, 2010. **9**(2): p. 369-78.
829   63.   Marathe, P.H., et al., *Preclinical pharmacokinetics and in vitro metabolism of*
830   *brivanib (BMS-540215), a potent VEGFR2 inhibitor and its alanine ester prodrug*
831   *brivanib alaninate.* Cancer Chemother Pharmacol, 2009. **65**(1): p. 55-66.

832

833

834   **Figure legends**

835

836   **Figure 1. ID1 is not a common downstream target of ENG in PMVECs.** A) Cartoon of

837   BMP9 signaling in HHT. B) Western blot verification of BMP9 in PMVECs. C-E) siRNA-

838   mediated knockdown verification of ALK1, ENG, and SMAD4 by qPCR. F and G)

839   Validation of BMP9 signaling in ALK1, ENG, and SMAD4 knockdown conditions in

840   PMVECs by qPCR (read out ID1).

841

Figure 2. Common downstream gene signatures of ALK1, ENG and SMAD4 mutations enriched for AVM and HHT related biological processes and cell signaling pathways. A and B) Venn diagram of common upregulated or downregulated genes following knockdown of ALK1, ENG and SMAD4 in PMVECs stimulated with BMP9 (20ng/ml) for 2 or 24hrs (RNAseq). C) Heatmap of the common upregulated and downregulated genes following knockdown of ALK1, ENG and SMAD4 in PMVECs stimulated with BMP9 for 2 and 24hrs. D) SinyGo biological processes analysis of the common upregulated and downregulated genes following knockdown of ALK1, ENG and SMAD4 in PMVECs stimulated with BMP9 for 2 and 24hrs. E) Panther pathway analysis of the common upregulated and downregulated genes following knockdown of ALK1, ENG and SMAD4 in PMVECs stimulated BMP9 for 2 and 24hrs.

853

Figure 3. Identifying common persistently dysregulated downstream gene signatures of the HHT gene knockdowns in PMVECs. A) Venn diagram of the common persistent upregulated and downregulated downstream gene signatures between 2 and 24 hrs of BMP9 stimulation following HHT gene knockdown. B) qRT-PCR validation of the common persistent upregulated and downregulated downstream gene signatures at 2 hrs of BMP9 stimulation following HHT gene knockdown. C) qRT-PCR validation of the common persistent upregulated and downregulated downstream gene signatures at 24 hrs of BMP9 stimulation following HHT gene knockdown.

862

Figure 4. Drug prediction based on the common upregulated downstream targets after ALK1, ENG and SMAD4 knockdown and experimental validation in PMVECs. A) Experimental strategy: the common upregulated genes 117 (2h) and 112 (24h) after knockdown of the three HHT genes and stimulation with BMP9 for 2 and 24hrs (HHT disease signature) were uploaded separately on the Clue query app. The criteria of the drugs rank include samples >=3, normalized connectivity score, tas value >=0.20, and FDR value. B) top scoring 5 HHT (positive values) and anti-HHT drugs (negative values, indicated by brown color) are represented. (C-K) Effect of Brivanib on the expression of the common persistent downstream targets (LYVE1, GPNMB, RRAGD, ANKRD33, HS3ST2, MC5R, SLC25A47, FGF19, SHISA9, FRG2C, HIST1H2BE, and CPA4) after ALK1, ENG and SMAD4 knockdown was assessed by qRT-PCR in PMVECs. MOA, mode of action; cs, connectivity score; tas, transcriptional activity score. Data are represented as mean ± standard error mean

875   (n=3). Two-way repeated measures ANOVA with a Bonferroni post-hoc test, *$P=<0.5$,

876   **$P=<0.01$, ***$P=<0.001$, ****$P=<0.0001$.

877

878   **Figure 5. Effect of Brivanib on expression of upregulated disease signature genes in**

879   **HHT in *ex vivo* healthy human PCLS.** A) PCLS protocol. B) Expression of LYVE1,

880   GPNMB, HS3ST2, RRAGD and ANKRD33 were measured by qRT-PCR following 24hrs

881   treatment of Brivanib in PCLS (B-F). Data are represented as mean ± standard error mean

882   (n=3). Unpaired Student's *t*-test, *$P=<0.5$.

883

884   **Figure 6. Brivanib inhibits VEGF-induced pERK1/2, -proliferation, and angiogenesis in**

885   **PMVECs.** A) PMVECs were treated with 10uM Brivanib or DMSO for 24 hrs followed by

886   20ng/mL VEGF or PBS for 10 mins. Protein was harvested and the effect of Brivanib on

887   VEGF-induced phosphorylation of ERK1/2 was assessed in PMVECs by western blotting. B)

888   The effect of Brivanib on VEGF-induced cell proliferation was assessed by MTT assay in

889   PMVECs. C) Angiogenesis was assessed in a Matrigel tube formation assay using PMVECs

890   treated with either Brivanib 1, 10, 50 uM or DMSO. D) Proposed model for the mechanism

891   by which Brivanib might influence AVM and HHT pathogenesis.

892

893   **Figure E1.** Functional consequence of ALK1, ENG, and SMAD4 knockdown in PMVECs

894   (proliferation, apoptosis and tube formation).

895

896   **Figure E2.** STRING network analysis of the common upregulated and downregulated genes

897   following knockdown of ALK1, ENG and SMAD4 in PMVECs stimulated with 2h and 24h

898   of BMP9.

899

900   **Figure E3.** Validation of common upregulated or downregulated genes signatures with

901   BMP9 stimulation at 2 (A and B) or 24 hrs (C and D) and functional consequences of the

902   knockdown of LYVE1, GPNMB and MC5R in PMVECs. After 72 hrs knockdown of

903   LYVE1, MC5R, and GPNMB PMVECs proliferation (E), apoptosis (F), tube formation (G)

904   were assessed.

905

906   **Figure E4.** Effect of Brivanib on the expression of the common persistent downstream

907   targets after ALK1, ENG and SMAD4 knockdown were assessed by qRT-PCR in PMVECs

908   (A-C).

909

910

911

912

913

914

915

916

917

918

919

920

921

922

923

924

925

926 **Figure 1**
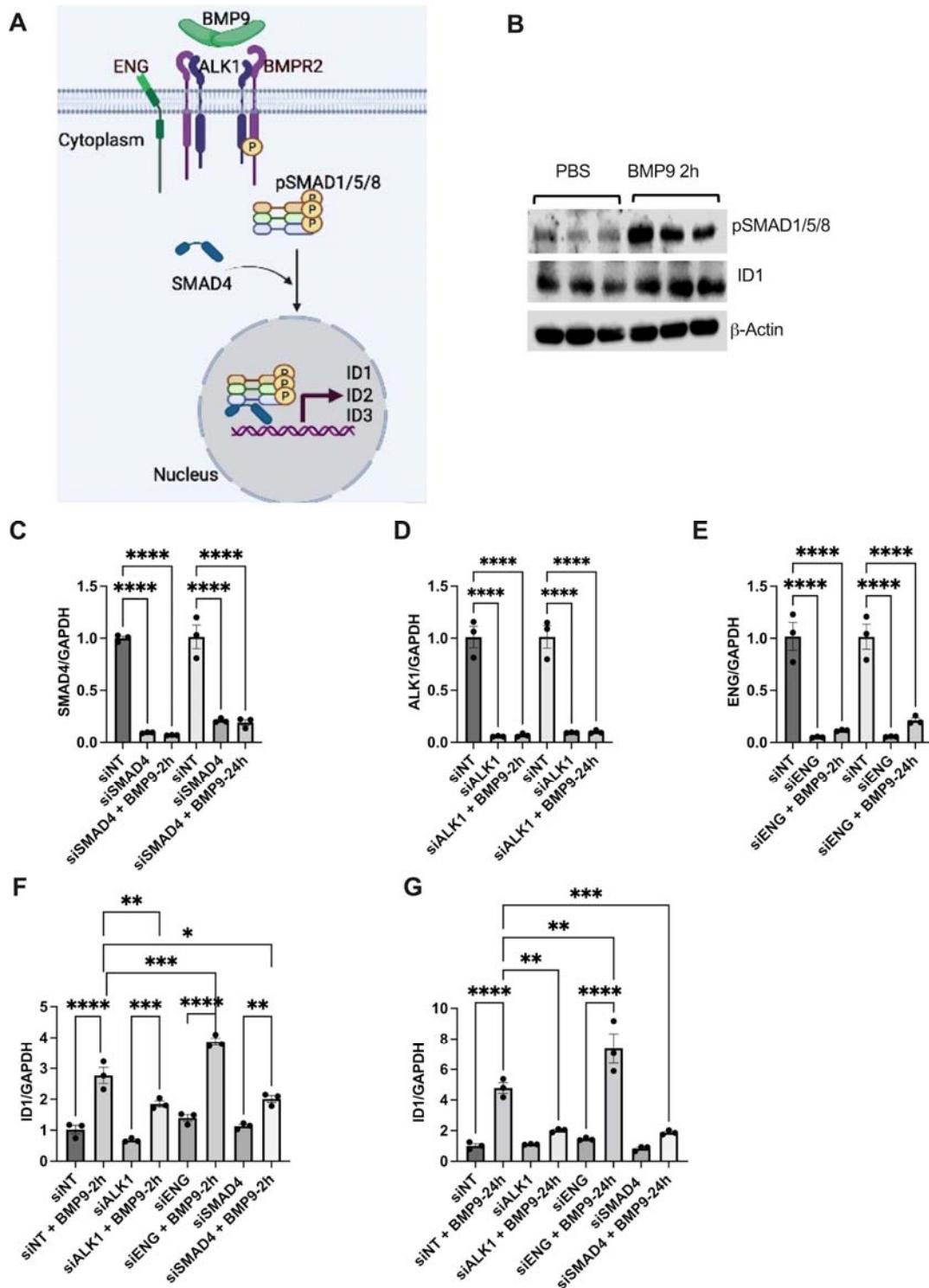
927

928

929

930

931 **Figure 2**

932

933

934

935

936
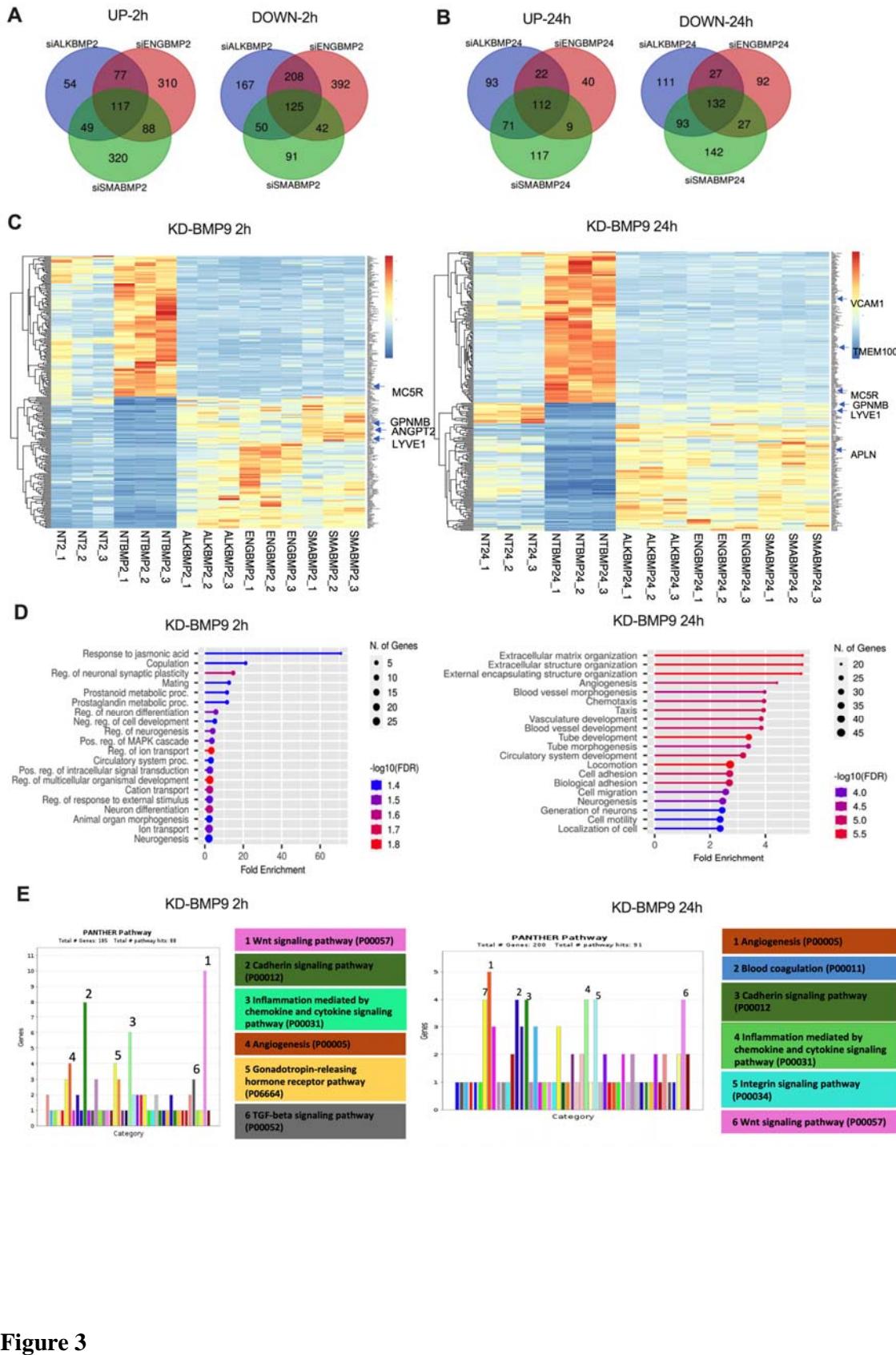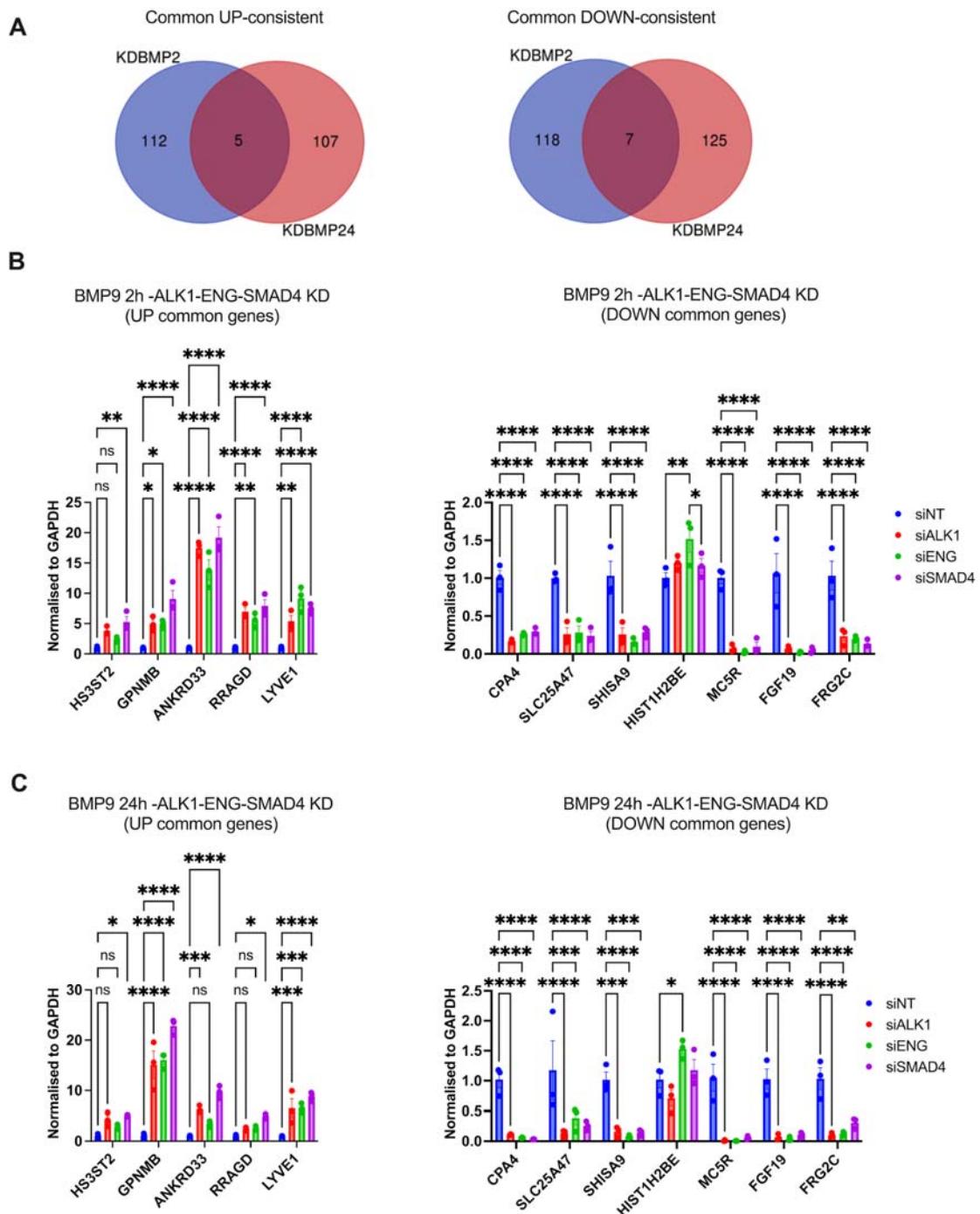
937 **Figure 3**

944 **Figure 4**

945
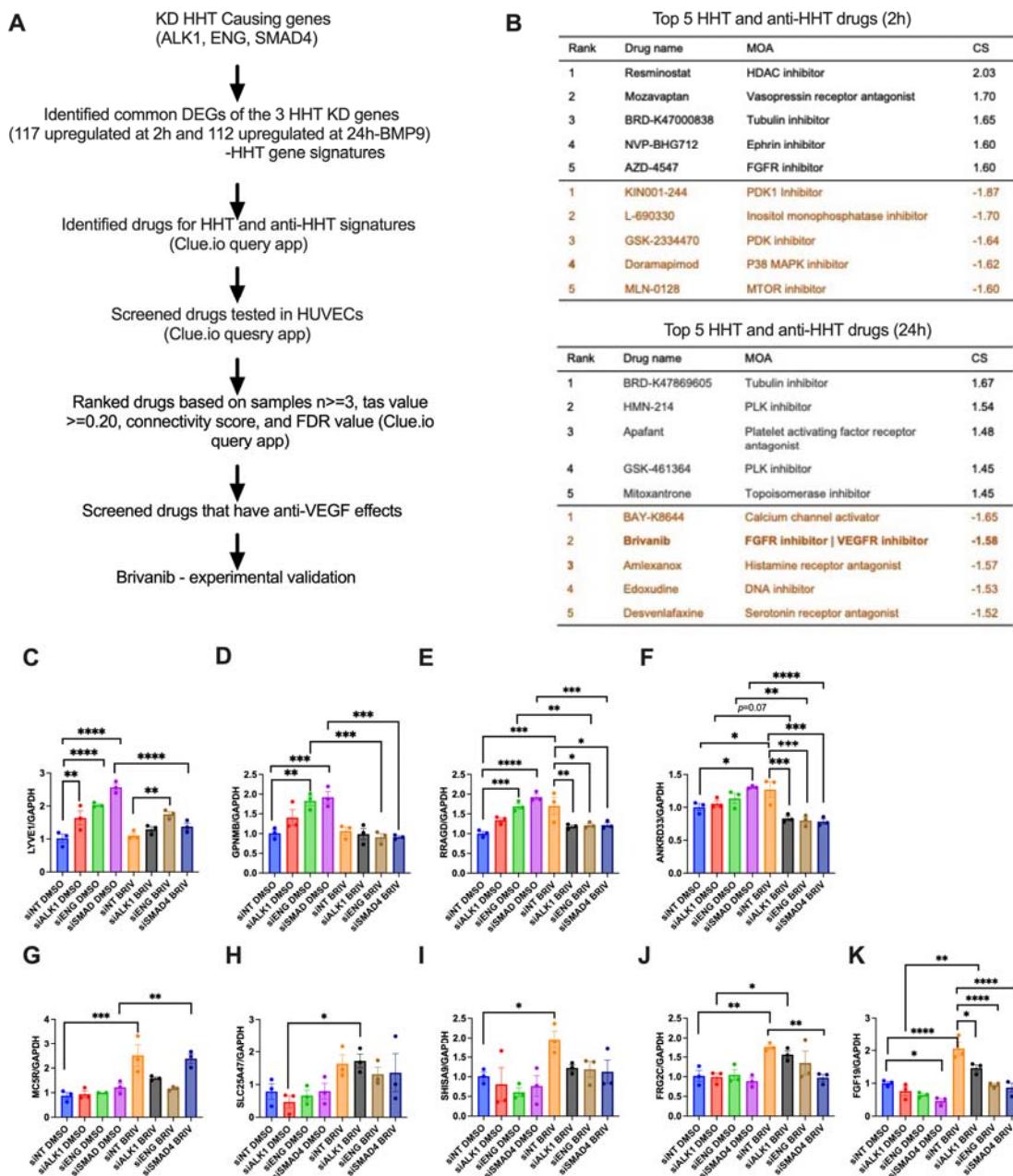
946
947
948
949
950
951
952
953 **Figure 5**
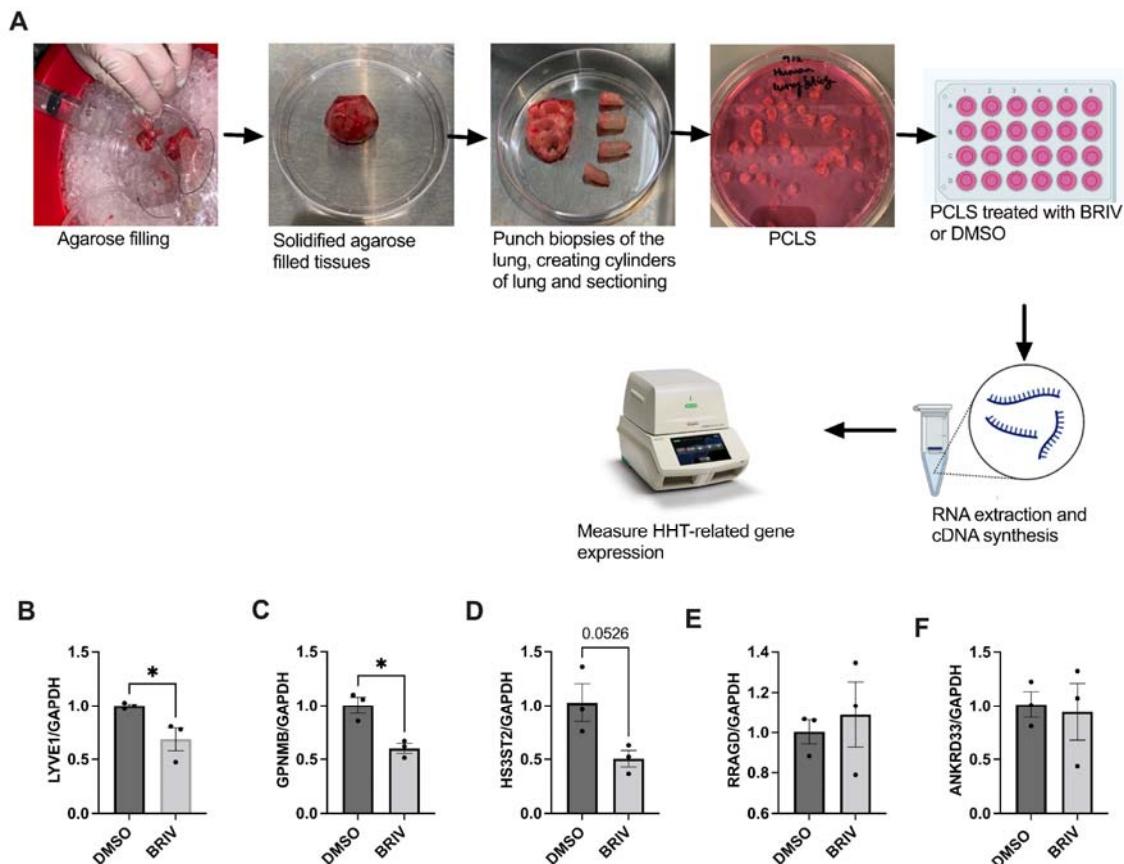
954

955

956

957

958

959

960

961

962

963

964

965

966

967

968

969

970 **Figure 6**
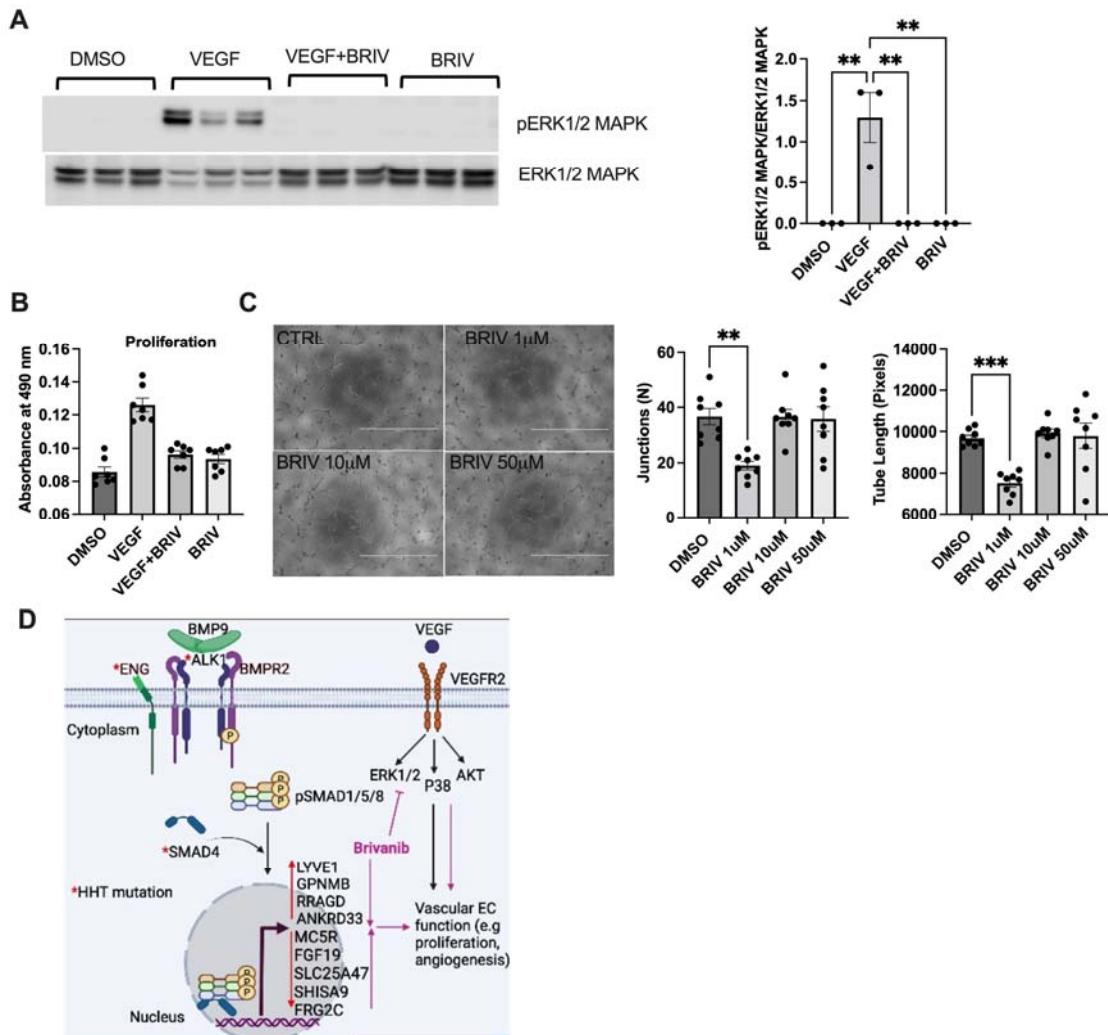
971

972

973

974

975

976

977

978

979

980

981

982

983

984   **Figure E1**
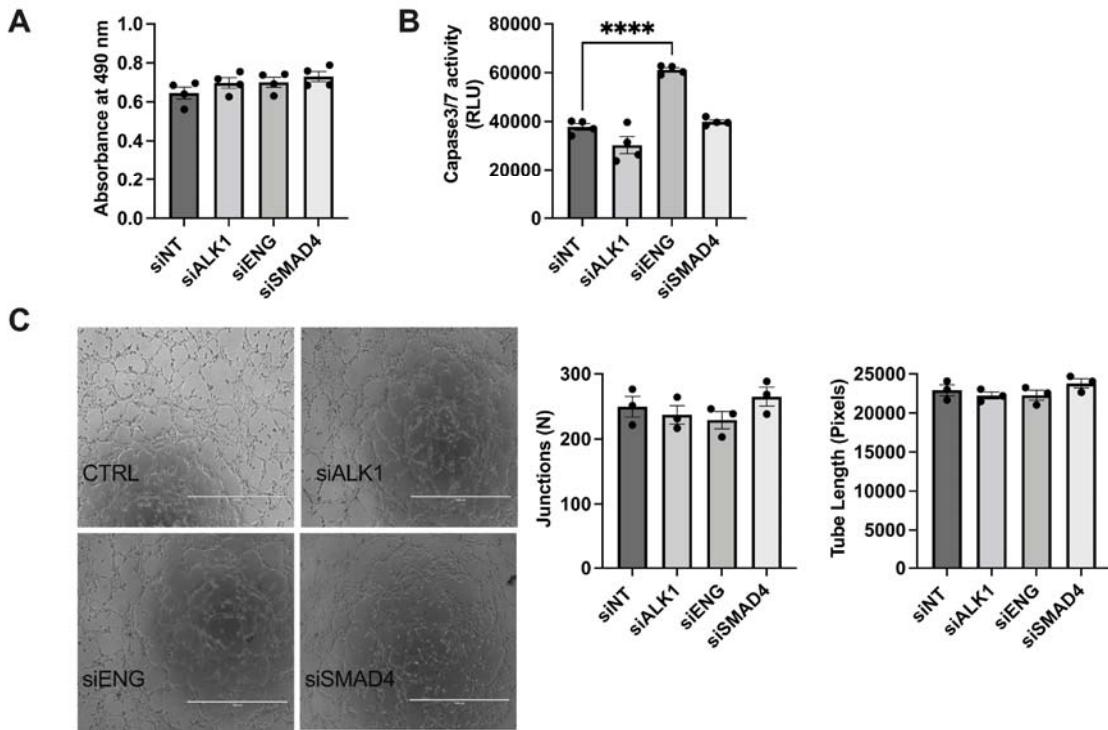
985
986
987
988
989
990
991
992
993
994
995
996
997
998
999
1000
1001
1002
1003
1004 **Figure E2**

A — STRING Network analysis KD BMP9 2h — proteins: 50 — interactions: 93 — expected interactions: 60 (p-value: 5.08e-05)
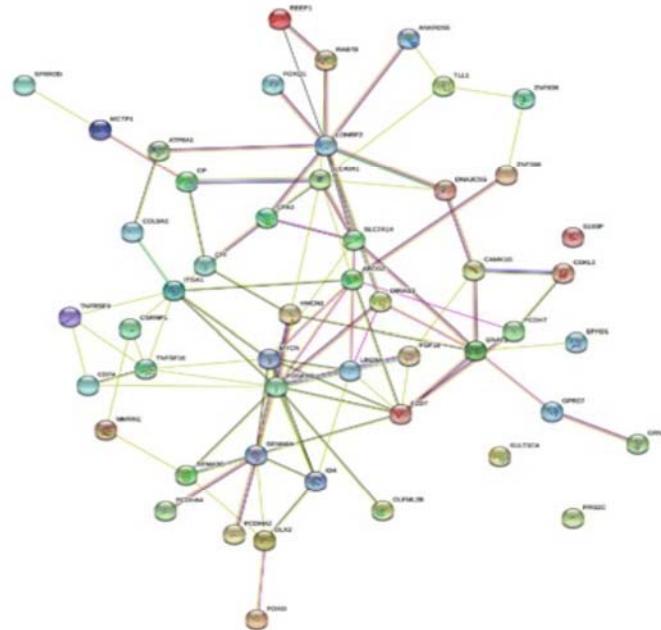
B — KD BMP9 24h — proteins: 50 — interactions: 110 — expected interactions: 54 (p-value: 1.49e-11)

1005

1006

1007 **Figure E3**

1008
1009
1010
1011
1012
1013
1014
1015 **Figure E4**

1016

1017

1018